Chapter 2

Proton Driver

2.1 The AGS as a Proton Driver

After more than 40 years of operation, the AGS is still at the heart of the Brookhaven hadron accelerator complex. This system of accelerators presently comprises a 200 MeV linac for the pre-acceleration of high intensity and polarized protons, two Tandem Van de Graaff for the pre-acceleration of heavy ion beams, a versatile Booster that allows for efficient injection of all three types of beams into the AGS and, most recently, the two RHIC collider rings that produce high luminosity heavy ion and polarized proton collisions. For several years now, the AGS has held the world intensity record with more than 7×10^{13} protons accelerated in a single pulse.

We describe here possible upgrades to the AGS complex that would meet the requirements for the proton beam driver for Neutrino Factory operation. Those requirements are summarized in Table 2.1 and a layout of the upgraded AGS is shown in Fig. 2.1. Since the present number of protons per fill is already close to the required number, the upgrade focuses on increasing the repetition rate and reducing beam losses (to avoid excessive shielding requirements and to maintain the ability to service machine components by hand). It is also important to preserve all the present capabilities of the AGS, in particular its role as injector to RHIC.

The AGS Booster was built not only to allow the injection of any species of heavy ion into the AGS, but to allow a fourfold increase of the AGS intensity. It is one-quarter the circumference of the AGS with the same aperture. However, the accumulation of four Booster loads in the AGS takes time, and is therefore not well suited for high average beam power operation. We are proposing here to build a superconducting upgrade to the existing 200 MeV linac to reach an energy of 1.2 GeV for direct H^- injection into the AGS. This will be discussed in Section 2.2. The minimum ramp time to full energy is presently 0.5 s; this must be upgraded to reach the required repetition rate of 2.5 Hz. Since the six bunches are extracted one bunch at a time, as is presently done for the operation of the g-2 experiment, a 100 ms flattop is included, which leaves only 150 ms for the ramp up or ramp down cycle. The required upgrade of the AGS power supply will be described in Section 2.3. Finally, the increased ramp rate and the final bunch compression require a substantial upgrade to the AGS rf system and improvements in the vacuum chamber as well. The rf upgrade will be discussed in Section 2.4.

Table 2.1: AGS proton driver parameters.

Total beam power (MW)	1
Beam energy (GeV)	24
Average beam current (μA)	42
Cycle time (ms)	400
Number of protons per fill	1×10^{14}
Average circulating current (A)	6
No. of bunches per fill	6
No. of protons per bunch	1.7×10^{13}
Time between extracted bunches (ms)	20
Bunch length at extraction, rms (ns)	3
Peak bunch current (A)	400
Total bunch area (eVs)	5
Bunch emittance, rms (eV-s)	0.3
Momentum spread, rms	0.005

The front end consists of a high intensity negative ion source, followed by a 750 keV RFQ, and the first five tanks of the existing room temperature Drift Tube Linac (DTL). The superconducting linac (SCL) is made of three sections, each with its own energy range and cavity cryostat arrangement.

The front end ion source operates with a 1% duty cycle at the repetition rate of 2.5 Hz. The beam current within a pulse is 37.5 mA of H^-. The ion source sits on a platform at 35 kV. The beam is prechopped by a chopper located between the ion source and the RFQ. The chopping extends over 65% of the beam length, at a frequency matching the accelerating rf at injection into the AGS. Transmission efficiency through the RFQ is taken conservatively to be 80%, so that the average current of the beam pulse in the linac, where we assume no further beam loss, is 20 mA, with a peak value of 30 mA. The

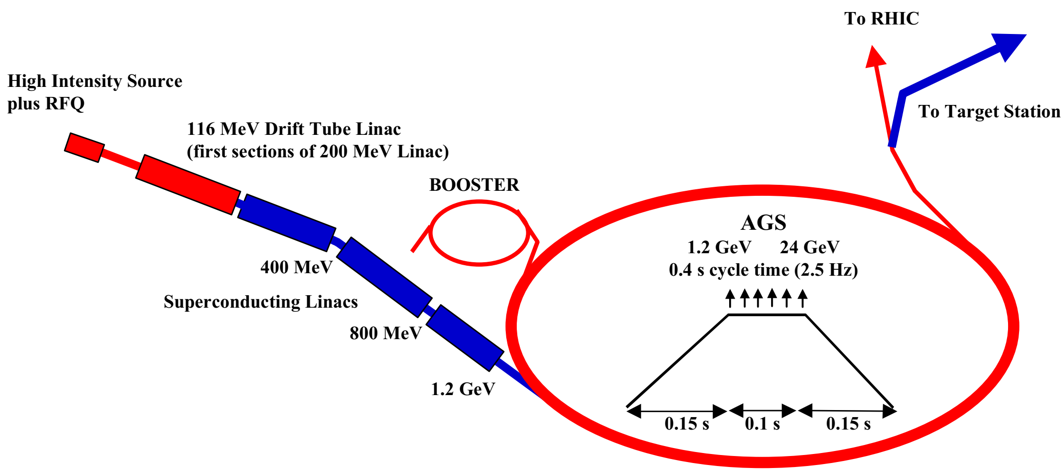

Figure 2.1: AGS proton driver layout.

combination of the chopper and the RFQ prebunches the beam with a sufficiently small bunch length that each beam bunch fits into an accelerating rf bucket of the downstream DTL, which operates at 201.25 MHz. The DTL is a room-temperature conventional linac that accelerates to 116 MeV.

The proposed new injector for the AGS adds a 1.2 GeV SCL with an average output beam power of about 50 kW. The injection energy is still low enough to control beam losses due to stripping of the negative ions that are used for multiturn injection into the the AGS. The duty cycle is about 0.5%. Injection into the AGS is modeled after the SNS scheme [1]. However, the repetition rate, and consequently the average beam power, is much lower here. The larger circumference of the AGS also reduces the number of foil traversals. Beam losses at injection into the AGS are estimated to be about 3% controlled losses and 0.3% uncontrolled losses. This is based on a comparison with the actual experience in the AGS Booster and the LANL PSR and the predicted losses at the SNS, using the quantity $\mathrm{N_P}\ /\beta^2\gamma^3$ A), which is proportional to the Laslett tune shift, as a scaling factor. This is summarized in Table 2.2. As can be seen, the predicted 3% beam loss is consistent with the AGS Booster and the PSR experience and also with the SNS prediction.

With the AGS rf harmonic number of 24, the Linac beam will be injected into 18 buckets, as discussed in Section 2.4. A bunch merge of 3 to 1 will take place later in the cycle to produce 6 bunches in the AGS.

The AGS injection parameters are summarized in Table 2.3. A relatively low rf voltage

Table 2.2: Comparison of H^- injection parameters.

	AGS Booster	SNS	PSR	1 MW AGS
Beam power, linac exit (kW)	3	1000	80	54
Kinetic energy (MeV)	200	1000	800	1200
No. of protons N_P (10^{12})	15	100	31	100
Vertical acceptance, A (π mm mrad)	89	480	140	55
$\beta^2\gamma^3$	0.57	6.75	4.50	9.56
$N_P/(\beta^2\gamma^3 A)$ ($10^{12}/\pi$ mm mrad)	0.296	0.031	0.049	0.190
Total beam losses (%)	5	0.1	0.3	3
Total lost beam power (W)	150	1000	240	1440
Circumference (m)	202	248	90	807
Lost beam power per meter (W/m)	0.8	4.0	2.7	1.8

of 450 kV at injection energy is necessary to limit the beam momentum spread during the multi-turn injection process to about 0.48%, and the longitudinal emittance to be about 1.2 eV-s per bunch. Such a small emittance is important to limit beam losses during transition crossing and to allow for effective bunch compression before extraction from the AGS.

A preliminary simulation of the 360-turn injection process is shown in Fig. 2.2. Without the second harmonic rf, some dilution in phase space of the injected particles is inevitable. The bunch shape is similar to that at the PSR in Los Alamos, with a noticeable sharp peak. A possible Linac beam momentum ramping could improve this if necessary.

Beam instability consideration are focused on two aspects. These are, for the AGS, the longitudinal instability around transition energy, and the transverse instability above transition, at high energy.

The fractional beam momentum spread at transition must be less than 0.0075 because of the limited momentum aperture during the transition-energy jump. With the transition jump, the slippage factor can be controlled to be greater than 0.002. With a bunch rms length of 4.25 ns and a peak current of 85 A at transition, the longitudinal impedance must be less than 11 Ω to avoid longitudinal microwave instability. An upgraded vacuum chamber to accomplish this is included in the baseline design.

The measured AGS broadband impedance is about 30 Ω. The broadband impedance mainly comes from the unshielded bellows, the vacuum chamber connections and steps, and cavities, and also has possible contributions from the BPMs and ferrite kickers. With

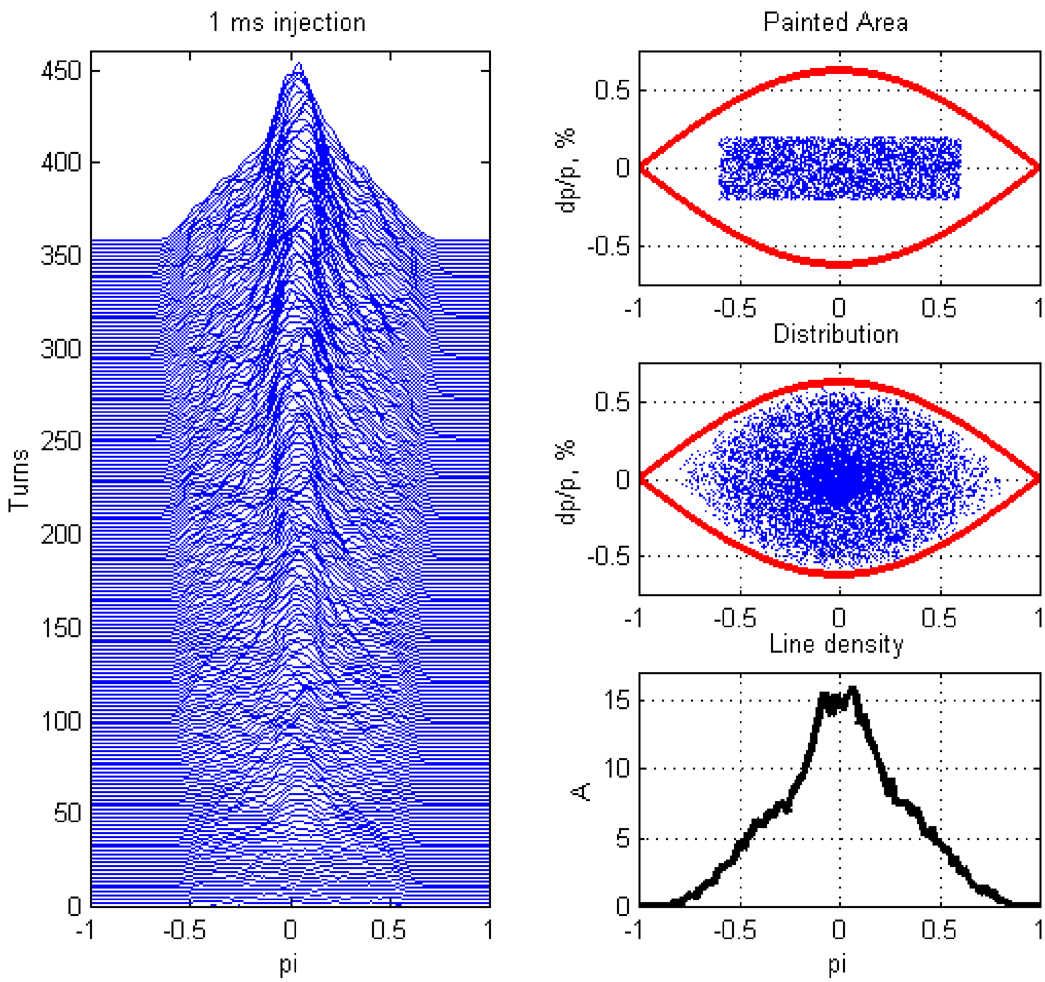

Figure 2.2: AGS injection simulation. The abscissa is phase.

Table 2.3: AGS injection parameters.

Injection turns	360
Repetition rate (Hz)	2.5
Pulse length (ms)	1.08
Chopping rate (%)	65
Linac average/peak current (mA)	20/30
Momentum spread	± 0.0015
Norm. 95% emittance ($\pi\mu$m $\cdot$ rad)	12
RF voltage (kV)	450
Bunch length (ns)	85
Longitudinal emittance (eV-s)	1.2
Momentum spread	± 0.0048
Norm. 95% emittance ($\pi\mu$m $\cdot$ rad)	100

a modest effort, this impedance can be reduced to be less than 10 Ω, which is consistent with newly designed proton machines.

In fact, if only the longitudinal microwave instability were of concern, a larger broadband impedance could be tolerated, since the longitudinal space-charge impedance of about 10 Ω at transition, which is capacitive, has the effect of canceling the inductive broadband impedance. However, the transverse instability at high energy is more serious, even with a broadband impedance of 10 Ω.

At 24 GeV, and with bunches compressed to 3 ns rms, each with an intensity of 1.7×10^{13} protons, the beam peak current reaches almost 400 A, which is about 7 times higher than the present running condition. With a transverse broadband impedance of 2.1 MΩ/m, scaled from the longitudinal impedance of 10 Ω, the coherent tune shift is then about 0.04, which implies an instability growth rate of 10 μs.

The space-charge incoherent tune spread, which is the main transverse microwave instability damping force at low energy, is reduced at high energy to a value comparable to 0.04. This is not sufficient to stabilize the beam. Other possible damping forces are discussed as follows. The slippage factor $\eta = 0.013$ at 24 GeV, together with the beam momentum spread of 0.01 for a bunch with 3 ns rms length, gives rise to a tune spread of 0.001, which is negligible. The chromatic tune spread with the chromaticity of 0.25 is 0.02, contributing only marginally to beam stability. Possibly the tune spread from octupoles or rf quadrupoles could stabilize the beam, but the choice of an improved vacuum chamber seems prudent.

Other issues are not as significant. For example, the space charge is not significant

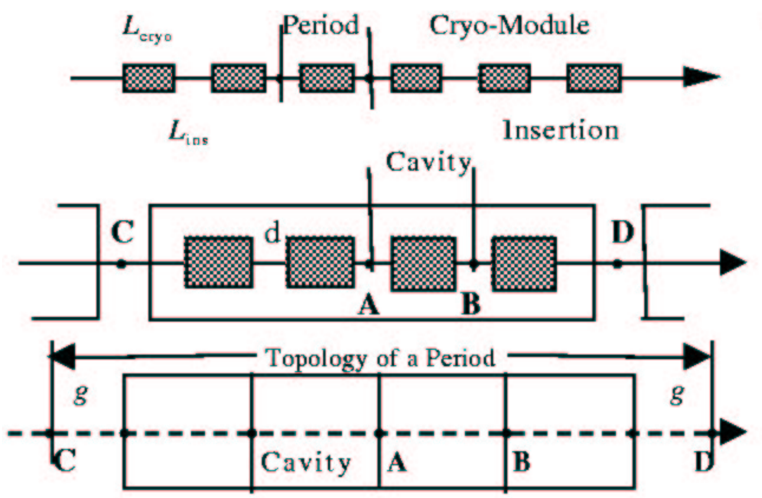

Figure 2.3: Configuration of the cavities within the cryo-modules (cryostats).

even for the compressed bunches and the beam momentum spread of ± 0.01 is well within the AGS momentum aperture at high energy.

In summary, since the intensity of 1×10^{14} is only marginally higher than the present intensity of 7×10^{13}, the beam instability during acceleration and transition crossing can be avoided. Transverse instability is likely to be the most dangerous during the bunch compression in the AGS ring, even with a reduced broadband impedance.

2.2 Superconducting Linac (SCL)

The SCLs accelerate the proton beam from 116 MeV to 1.2 GeV. The configuration we use follows a design similar to that described in Ref. [2]. All three linacs are built up from a sequence of identical periods, as shown in Fig. 2.2. Each period comprises a cryomodule and a room-temperature insertion that is needed for the placement of focusing quadrupoles, vacuum pumps, steering magnets, beam diagnostic devices, bellows and flanges. Each cryomodule includes four identical cavities, each with four or eight identical cells.

The choice of cryomodules with identical geometry, and with the same cavity/cell configuration, is economical and convenient for construction. Still, there is a penalty due to the reduced transit–time factors when a particle crosses cavity cells with lengths adjusted to a common central value β_o that does not correspond to the particle's in-

Table 2.4: Parameters of the superconducting linacs.

	Low energy	Medium energy	High
Beam power, linac exit (kW)	16	32	48
Kinetic energy range (MeV)	116 - 400	400 - 800	800 - 1200
Velocity range, β	0.4560 - 0.7131	0.7131 - 0.8418	0.8418 - 0.8986
Frequency (MHz)	805	1610	1610
Protons per bunch (10^8)	9.32	9.32	9.32
Temperature (K)	2.0	2.0	2.0
Cells per cavity	4	8	8
Cavities per cryo-module	4	4	4
Cell length (cm)	9.68	6.98	8.05
Cell reference velocity, β_o	0.520	0.750	0.865
Cavity internal diameter (cm)	10	5	5
Cavity separation (cm)	32	16	16
Cold-to-warm transition (cm)	30	30	30
Accelerating gradient (MV/m)	11.9	22.0	21.5
Cavities per klystron	4	4	4
No. of klystrons (or periods)	18	10	9
Klystron power (kW)	720	1920	2160
Energy gain per period (MeV)	16.0	42.7	48.0
Length of period (m)	4.2	4.4	4.7
Total length (m)	75.4	43.9	42.6

stantaneous velocity. This is the main reason to divide the superconducting linac into three sections, each designed around a different central value β_o, and, therefore, having different cavity/cell configurations. The cell length in a section is fixed to be $l\frac{\beta_o}{2}$ where l is the rf wavelength.

The major parameters of the three sections of the SCL are given in Table 2.4. The low-energy section operates at 805 MHz and accelerates from 116 to 400 MeV. The following two sections, accelerating to 800 MeV and 1.2 GeV, respectively, operate at 1.62 GHz. A higher frequency is desirable for obtaining a larger accelerating gradient with a more compact structure and reduced cost. Transverse focusing is done with a sequence of FODO cells with halflength equal to that of a period. The phase advance per cell is 90°. The rms normalized betatron emittance is $\approx 0.3\ \pi$ mm mrad. The rms bunch area is 0.5π MeV-deg. The rf phase angle is 30°. The length of the linac depends on the average accelerating gradient, which has a maximum value that is limited by three causes:

1. The surface-field limit at the frequency of 805 MHz, taken to be 26 MV/m. For a realistic cavity shape, we set a limit of 13 MV/m on the axial electric field. For the following two sections, the surface-field limit at 1.61 GHz is 40 MV/m and, correspondingly, we adopt a limit of 20 MV/m on the axial electric field.

2. The rf coupler power limit, which we take here not to exceed 400 kW (including a contingency of 50% to avoid saturation effects).

3. The need to make the longitudinal motion stable, which limits the energy gain per cryomodule to a small fraction of the beam energy [2].

The proposed mode of operation is to run each section of the SCL with the same rf input power per cryomodule. This will result in some variation of the actual axial field from one cryomodule to the next. A constant value of the axial field, if needed, could be obtained by locally adjusting the value of the rf phase.

For a pulsed mode of operation of the superconducting cavities, the Lorentz forces could deform the cavity cells enough to tune them off resonance. This is controlled with a thick cavity wall and additional supports. Also, a significant time to fill the cavities with rf power is required before the maximum gradient is reached and beam can be injected. The expected filling time is short compared with the beam pulse length of 1 ms.

2.3 AGS Main Power Supply Upgrade

2.3.1 Present Mode of Operation

The present AGS Main Magnet Power Supply (MMPS) is a fully programmable 6000 A, ±9000 V SCR power supply. A 9 MW Motor Generator (MG), made by Siemens, is a part of the main magnet power supply of the accelerator. The MG permits pulsing the main magnets up to 50 MW peak power, while the input power of the MG itself remains constant. The highest power into the MG ever utilized is 7 MW, that is, the maximum average power dissipated in the AGS magnets has never exceeded 5 MW.

The AGS ring comprises 240 magnets connected in series. The total resistance, R, is 0.27 Ω and the total inductance, L, is 0.75 H. There are 12 superperiods, designated A through L, of 20 magnets each, divided in two identical sets of 10 magnets per superperiod.

Two stations of power supplies are each capable of delivering up to 4500 V and 6000 A. Every station consists of two power supplies connected in parallel. One power supply is a 12-pulse SCR unit (P type) rated at ±5000 V, 6000 A, that is typically used for fast ramping during acceleration and energy recovery. The other is a lower voltage 24 pulse unit (F type), rated at ±1000 V, 6000 A, that is used for flattop or slow ramping operation. The two stations are connected in series, with the magnet coils arranged to have a total resistance $R/2$ and a total inductance of $L/2$. The grounding of the power supply is done only in one place, in the middle of station 1 or 2, through a resistive network. With this grounding configuration, the maximum voltage to ground in the magnets does not exceed 2500 V. The magnets are tested at 3 kV to ground prior to each startup of the AGS MMPS after long maintenance periods.

2.3.2 Neutrino Factory Mode of Operation

To cycle the AGS ring to 24 GeV at 2.5 Hz and with a ramp time of 150 ms, the magnet peak current is 4300 A and the peak voltage is 25 kV. Figure 2.4 displays the magnet current and voltage of a 2.5 Hz cycle. The cycle includes a 100 ms flat-top for the six single-bunch extractions. The total average power dissipated in the AGS magnets is estimated to be 3.7 MW. To limit the AGS coil voltage to ground to 2.5 kV, the AGS magnets must be divided into three identical sections, each powered similarly to the present AGS except that now the magnet loads represent only 1/6 of the total resistance and inductance. Every section will be powered separately with its own feed to the ring magnets and an identical system of power supplies, as shown in Fig. 2.5. Bypass SCRs will be used across the four new P-type stations, to bypass these units during the flat-top, and ensure minimum ripple. Note that only station 1 will be grounded, as done presently. Although the average power will not be higher than now, the peak power required is approximately 110 MW, exceeding the 50 MW rating of the existing MG. A new MG, capable of providing 100 MW, would operate with 12 phases to limit, or even eliminate, the need for phase-shifting transformers, so that every power supply system would generate 24 pulses. The generator voltage will be about 15 kV line-to-line, to limit the generator current to less than 6000 A during pulsing. The generator will be rated at a slip frequency of 2.5 Hz.

Running the AGS at 2.5 Hz requires that the acceleration ramp period decreases from 0.5 s to 0.15 s. That is, the magnet current variation dI/dt is about 3.3 times larger than at present. Eddy current losses in the vacuum chamber are proportional to the square of *(dI/dt)*, that is, they are 10 times larger. However, this is still significantly below the present ramp rate of the AGS Booster which does not require active cooling. The increased eddy currents give rise to increased sextupole fields during the ramp, and will add about 20 units of chromaticity. The present chromaticity sextupoles will be upgraded to correct this and the upgraded vacuum chamber will also mitigate the effects of the faster cycle.

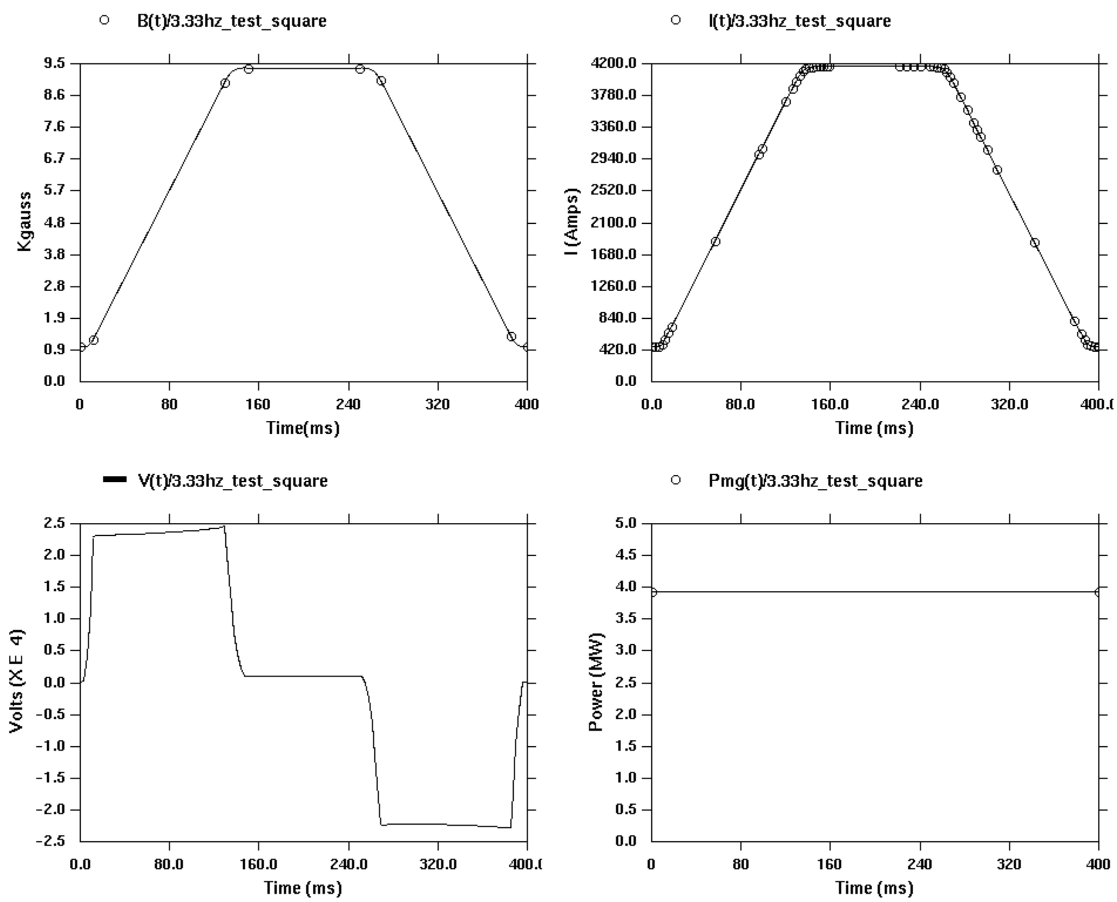

Figure 2.4: Current and voltage cycle for 2.5 Hz operation. Also shown are the AGS dipole field and average power.

2.4 AGS rf System Upgrade

At 2.5 Hz, the peak acceleration rate is three times the present value for the AGS. With 10 accelerating stations, each station will need to supply 270 kW peak power to the beam. The present power amplifier design, employing a 300 kW power tetrode will be suitable to drive the cavities and supply power to the beam. The number of power amplifiers will be doubled, so that each station will be driven by two amplifiers of the present design. This follows not so much from power considerations but from the necessity to supply 2.5 times the rf voltage.

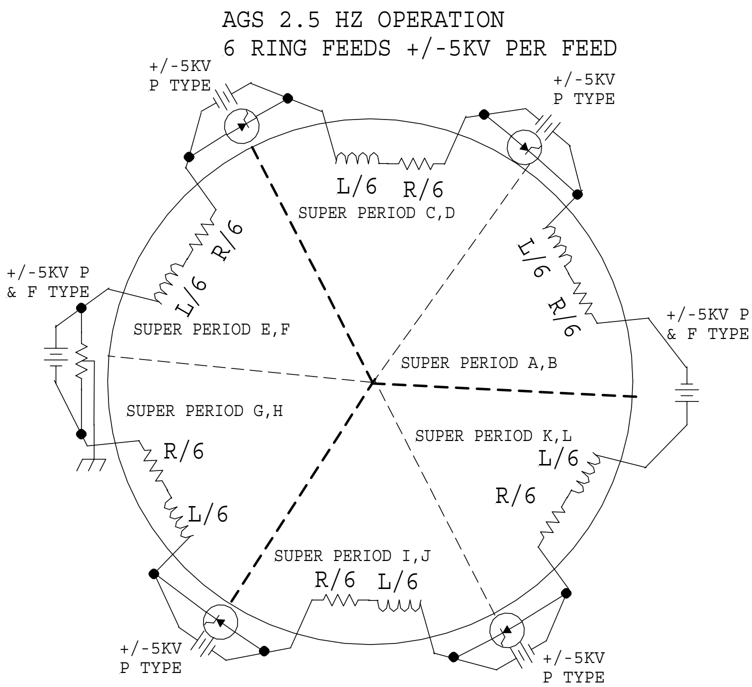

Figure 2.5: Schematic of power supply connections to the AGS magnets for 2.5-Hz operation.

An AGS rf station comprises four acceleration gaps surrounded by 0.35 m of ferrite stacks. The maximum voltage capability of a gap is not limited by the sparking threshold of the gap, but by the ability of the ferrite to supply the magnetic induction. When the AGS operates at 0.5 Hz, the gap voltage is 10 kV. At 2.5 Hz, we will need up to 25 kV per gap (roughly equal to the voltage from the same gap design used at the Booster, 22.5 kV) and this taxes the properties of the ferrite. Above a certain threshold value of B_{rf} (20 mT for AGS ferrite 4L2) a ferrite becomes unstable and excessively lossy. The gap voltage at this $B_{rf,max}$ is simply given by

$$V = -\frac{d}{dt}\int \omega B_{rf} dA = \omega a l B_{rf,max} \ln\frac{b}{a} \tag{2.1}$$

where ω is the rf angular frequency and the variables a, b, and l are the inner and outer radius and length of the ferrite stack, respectively.

The only free variable is ω. If we operate the rf system at the 24th harmonic of the revolution frequency (9 MHz) then the required voltage of 25 kV can be achieved with a safe value for $B_{rf,max}$ of 18 mT.

The next issue is the power dissipation in the ferrite and the thermal stress that is created by differential heating due to rf losses in the bulk of the material. We know from experience that below 300 mW/cm^3 the ferrites can be adequately cooled. The power density is also proportional to B_{rf}^2 and is given by

$$\frac{P}{V} = \frac{\omega B_{rf}^2}{2\mu_0(\mu Q)} \tag{2.2}$$

where μQ is the quality factor of the ferrite.

The μQ product is a characteristic of the ferrite material and depends on frequency and B_{rf}. We have data on ferrite 4M2 (used in the Booster and SNS) at 9 MHz and 20 mT where the power dissipation is 900 mW/cm^3. The details of the acceleration cycle determine the rf voltage program that is needed. For the cycle shown in Fig. 2.4, a peak voltage of 1 MV (40 gaps each with 25 kV) is needed but for only 20 ms during acceleration. An additional 100 ms operation at 1 MV is required for the bunch compression. Together, this is a duty factor of less than 0.3, giving an average power dissipation below our limit. We do not yet have data on the present AGS ferrite, 4L2 at 9 MHz. Characterizing 4L2 in this parameter regime is identified as an R&D issue, but we know that retrofitting the AGS cavities with 4M2 is a viable fallback option.

With the rf system operating on harmonic 24, there will be 24 rf buckets. However, we need all the beam in 6 bunches to extract to the production target. This can be arranged by filling 18 of the 24 buckets with 6 triplets of bunches, as shown in Fig. 2.6. The fast chopper in front of the linac can prepare this bunch pattern during the multi-turn injection as described in Section 2.1. The fast chopper fills the buckets to a longitudinal emittance of 1.2 eV-s which can be accelerated with 1 MV/turn of rf voltage, allowing some blowup during the acceleration cycle. At the end of the acceleration cycle, the triplets will be merged adiabatically into 6 single bunches [3] using separate 100 kV/turn harmonic 6 rf cavities. The final bunch emittance would be at least 5 eV-s per bunch after the 3:1 bunch merge.

With 100 kV/turn of the harmonic 6 rf system, the total bunch length will be 80 ns for a 5 eV-s bunch. The rf system will then be switched back to harmonic 24 and 1 MV/turn, where the bunch is now mismatched. By strongly modulating the rf voltage with a frequency close to twice the synchrotron frequency of 512 Hz, the tumbling bunch can be kept from decohering. Also, the quadrupole oscillation frequency of the bunch can be controlled so that the bunch length is minimal at the times of the 6 bunch extractions [4]. The minimal total bunch length is about 15 ns, or 3 ns rms. This is about half of the

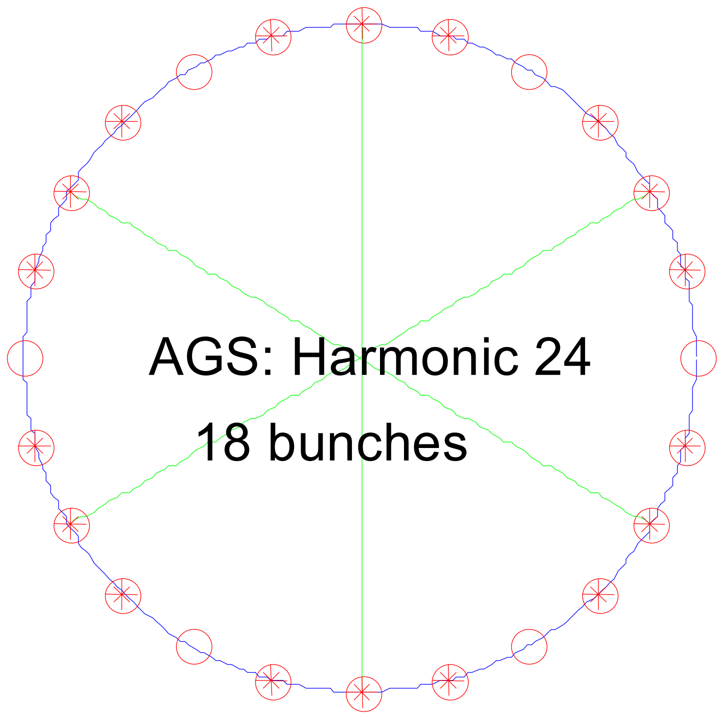

Figure 2.6: Bunch pattern for using harmonic 24 to create 6 bunches.

matched total bunch length of 32 ns.

2.5 Conclusions

The scheme for a 1-MW proton driver based on the AGS with upgraded injection is feasible. Indeed, the AGS beam intensity is only modestly higher than during the present high-intensity proton operation and, therefore, beam instability is not expected to be a problem during acceleration. Beam stability during the bunch compression is marginal, and requires some care to reach the 3 ns bunch length specification.

Bibliography

[1] J. Wei *et al.*, *Low-loss design for the high-intensity accumulator ring of the Spallation Neutron Source*, Phys. Rev. ST Accel. Beams 3, 080101 (2000).

[2] A. Ruggiero, *Design Considerations on a Proton Superconducting Linac*, BNL Internal Report 62312, 1995.

[3] R. Garoby, *Bunch Merging and Splitting Techniques in the Injectors for High Energy Hadron Colliders*, CERN/PS 98-048.

[4] M. Bai *et al.*, *Adiabatic excitation of longitudinal bunch shape oscillations*, Phys. Rev. ST Accel. Beams 3, 064001, 2000.